NURETH14-242

APPLICATION OF WAVELET TRANSFORMS AS A TIME-SERIES ANALYSIS TOOL FOR NUCLEAR THERMALHYDRAULICS

D.J. Pohl, J. Pascoe and A.I. Popescu

AMEC NSS Limited, Toronto, Ontario, Canada daniel.pohl@amec.com, jason.pascoe@amec.com, adrian.popescu@amec.com

Abstract

Wavelet transforms can be a valuable time-series analysis tool in the field of nuclear thermalhydraulics. As an example, the Morlet wavelet transform can be used to reduce the aleatory (random) uncertainty of a voiding transient in a large loss of coolant accident (LOCA). The wavelet transform is used to determine the cutoff frequency for a low pass Butterworth filter in order to remove the noisy part of the signal without infringing upon the characteristic frequencies of the phenomenon. This technique successfully reduced the standard random uncertainty by 42.4%.

Introduction

Wavelet analysis has recently become a popular tool in the geosciences for analyzing localized variations of power within time-series [1]-[3]. Using the wavelet transform, one is able to determine both the dominant modes of variability and how those modes vary in time by decomposing the time-series into the time-frequency domain. The wavelet transform uses base functions called wavelets that have smooth ends to perform the decomposition. As the name implies, wavelets are small wave packets that can be stretched and translated with a flexible resolution in both frequency and time, which allow them to easily map changes in the time-frequency domain. Mathematically speaking, a wavelet transformation decomposes a time-series into some elementary functions from a mother wavelet by dilation and translation. There are many mother wavelets available in literature, such as the Marr wavelet, the Paul wavelet and the Morlet wavelet. The Morlet wavelet is known to be the most popular wavelet used in the geosciences [1].

Wavelet analysis can also be a valuable time-series analysis tool in the field of nuclear thermalhydraulics, and can specifically aid best estimate plus uncertainty (BEPU) methods. Transient nuclear thermalhydraulic phenomena are characterized by their variation in time. These phenomena are understood by analyzing the time-series or signal of a parameter of interest.

An important accident within the field of nuclear thermalhydraulics is the loss of coolant accident (LOCA), which leads to coolant voiding. Within a CANDU nuclear reactor, coolant voiding within a fuel channel can lead to heat-up and damage of the fuel. Instrument measurements, including void fraction measurements, are subjected to high uncertainties. Measurements are often taken as the best estimates of true values, against which computer code calculations are compared. Hence, reducing the uncertainty of measurements will allow for better understanding of the uncertainties within the computer codes as well.

The overall uncertainty in any one measurement can be decomposed into two different types of uncertainties: aleatory (random) uncertainty and epistemic (systematic) uncertainty. A specific uncertainty reduction technique, aimed at reducing the aleatory uncertainty, involves the application

of a band-pass filter in order to remove the noisy part of the signal. The choice of the passband should not infringe upon the characteristic frequencies of the phenomenon being studied but should remove the noisy part of the signal as much as possible. The wavelet transform offers an advantage here, in that it allows the signal to be viewed simultaneously in both frequency and time therefore allowing one to easily choose the passband for a filter.

The objective of this study is to demonstrate the use of wavelet analysis in selecting a cutoff frequency for a band-pass filter, which will be used to reduce the aleatory uncertainty of a measurement. Specifically, the Morlet wavelet will be used to select cutoff frequency for a low pass Butterworth filter, which is in turn used to reduce the uncertainty of idealized void fraction data.

1. Nuclear Thermalhydraulic Time-Series Data

Transient nuclear reactor thermalhydraulic phenomena can be characterized by their variation in time. To better understand a given phenomenon, measurements of a parameter of interest are made and analyzed. However, every measurement has error, which results in a difference between the measured value and the true value. Ultimately, this places a limit on the degree to which a given phenomenon can be predicted.

1.1 Idealized Void Fraction Data Set

An important accident within the field of nuclear reactor thermalhydraulics is a loss of coolant accident (LOCA), which leads to a coolant voiding transient. The coolant void fraction can be characterized by:

$$\alpha = \frac{V_g}{V_\sigma + V_I} \tag{1}$$

where.

 α = is the coolant void fraction.

 V_{σ} = is the volume of the channel occupied by the coolant vapour phase, and

 V_{i} = is the volume of the channel occupied by the coolant liquid phase.

Coolant void fraction measurements were made during LOCA tests at the RD-14M experimental facility. Specifically, test B9401 shows voiding trends for a large LOCA. The heated section in the broken pass went from no voiding to complete voiding within approximately 10 seconds from the start of the break [5]. The RD-14M void fraction measurements are stated to be within $\pm 10\%$ void (95% confidence interval) [6].

Three distinct periods can be observed in the RD-14M LOCA test B9401 coolant voiding transients [5]:

- 1. Before the break: a minimum void fraction of 0.0 is sustained.
- 2. 0 to 10 seconds after the break: an approximately linear increase in void fraction from minimum value of 0.0 at the time of the break, to a value of 1.0 at 10 seconds.
- 3. >10 seconds after the break: a maximum void fraction value of 1.0 is sustained.

Using these characteristics and a break time of 55 seconds, an idealized void fraction time-series data set was constructed (see Figure 1). This data is used to represent the true value of coolant void fraction.

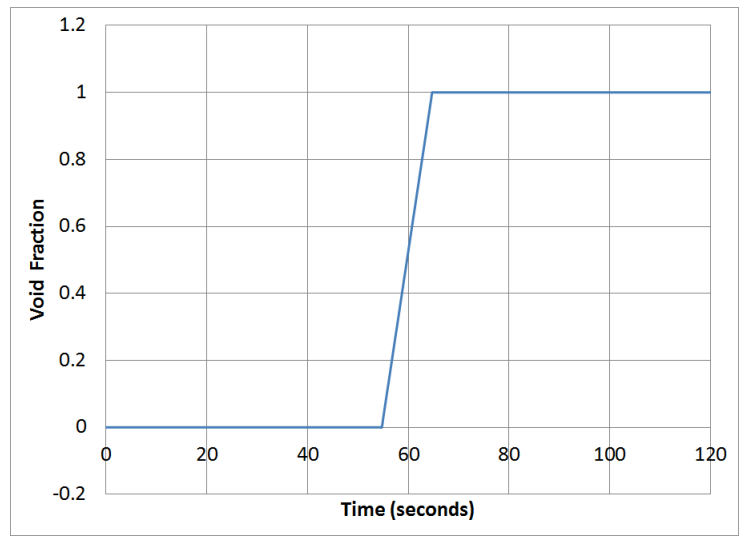


Figure 1: Idealized Coolant Void Fraction Transient - "True" Coolant Void Transient Fraction

In order to construct a data set for the "measured" value of coolant void fraction, a random uncertainty of $\pm 10\%$ void was added to the idealized "true" value (see Figure 2). In other words, what is referred to as the "measured" void fraction is actually an artificially created dataset.

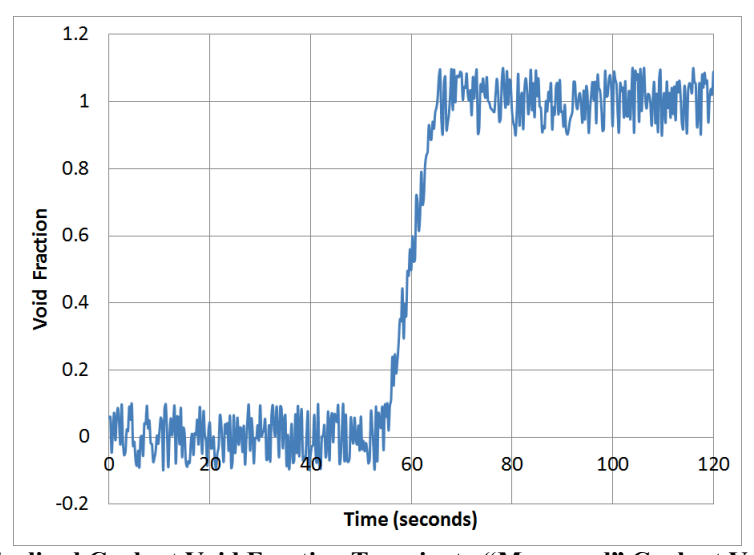


Figure 2: Idealized Coolant Void Fraction Transient - "Measured" Coolant Void Fraction

1.2 Measurement Uncertainty

There is an inherent uncertainty in the use of measurements to represent the true value. The total uncertainty in a measurement can be attributed to: uncertainty due to random error (aleatory) and uncertainty due to systematic error (epistemic) [4]. This paper will focuses on a technique to reduce the former.

In successive measurements of a parameter, e.g., void fraction, the values of elemental random error sources change resulting from random scatter. For measurements with zero systematic error, the mean is equal to the true value of the parameter and standard deviation is a measure of the scatter of the individual measurements about the mean. The sample mean is given by:

$$\overline{X} = \frac{\sum_{j=1}^{N} X_j}{N},\tag{1}$$

where,

 \overline{X} = is the sample mean,

 X_i = is the value of jth measurement, and

N = is number of measurements in the sample.

The sample standard deviation, s_X , is given by:

$$s_X = \sqrt{\sum_{j=1}^{N} \frac{(X_j - \overline{X})^2}{N - 1}},$$
 (2)

The random standard uncertainty of the sample mean, $s_{\overline{y}}$, is given by:

$$S_{\overline{X}} = \frac{S_X}{\sqrt{N}},\tag{3}$$

For a normally distributed population and a large same size, the interval $\overline{X} \pm 2 s_{\overline{X}}$ is expected to contain the true population mean with 95% confidence. The value of 2 represents the Student's t-value for 95% confidence and degrees of freedom, i.e., N-1 greater than or equal to 30.

1.3 Band-pass Filtering

A specific uncertainty reduction technique, aimed at the reducing the random standard uncertainty, involves the application of a band-pass filter in order to remove the random or "noisy" part of the signal. The choice of the passband should not infringe upon the characteristic frequencies of the phenomenon being studied but should remove the noisy part of the signal as much as possible. The wavelet transform, by decomposing the signal into the frequency-time domain, allows one to easily choose the passband frequency for a filter.

Many filter options are available within the Scilab software package. The Butterworth filter is a type of signal processing filter designed to have frequency response that is as flat as possible in the passband [7]. The Butterworth filters in Scilab are considered analog filters which are generally defined in the frequency domain as rational transfer functions of the form:

$$H(s) = \frac{\sum_{i=0}^{m} b_i s^i}{1 + \sum_{i=0}^{n} a_i s^i},$$
(4)

This is used to design an order n low pass digital Butterworth filter with normalized cutoff frequency, ω_c . Scilab returns the filter coefficients a_i and b_i or equivalently the zeros z_i and p_i poles of H in

order to meet given specifications of the magnitude response. A fourth-order low pass digital Butterworth filter was chosen for the voiding transient. Other band-pass filters may be used; however, it is important that the selected filter does not infringe up the frequencies of the phenomena understudy.

2. Wavelet Analysis

This section describes the method of wavelet analysis used for random uncertainty reduction, which has been adapted from the work of Trauth [1], Torrence and Compo [2], and Lau and Weng [3]. The wavelet software used was adapted from that provided by Torrence and Compo [8].

2.1 Wavelet Transform

A wavelet transform can be used to analyze a time-series that contains a non-stationary power at many different frequencies [2]. It uses base functions, i.e., wavelets, which can be dilated and translated with a changeable resolution in both frequency and time. An example being the Morlet wavelet, consisting of a plane wave modulated by a Gaussian [1]:

$$\psi_0(\eta) = \pi^{-1/4} e^{i\omega_0 \eta} e^{-\eta^2/2},\tag{5}$$

where,

 $\psi_0(\eta)$ = is the wavelet function,

 η = is the non-dimensional time parameter, and

 ω_0 = is the non-dimensional frequency.

The Morlet wavelet is the most popular wavelet used for time-series analysis in the geosciences [1] and is shown in Figure 3.

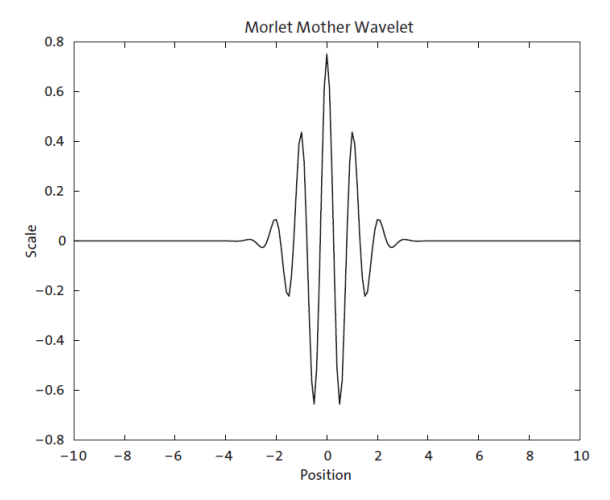


Figure 3: Morlet mother wavelet with wavenumber 6 [1]

Assuming that one has a time series, x_n , with equal time spacing, δt , and n = 0,..., N-1 the continuous wavelet transform is defined as the convolution of x_n with a scaled and translated version of $\psi_0(\eta)$:

$$W_n(s) = \sum_{n=0}^{N-1} x_n \psi * \left[\frac{(n'-n)\delta t}{s} \right], \tag{6}$$

where,

The 14th International Topical Meeting on Nuclear Reactor Thermalhydraulics, NURETH-14 Toronto, Ontario, Canada, September 25-30, 2011

 $W_n(s)$ = is the continuous wavelet transform,

N =is the total number of values in the time-series,

 x_n = is the time-series,

 ψ^* = is the complex conjugate of the wavelet function,

n = is the localized time index, δt = is the time spacing, and

s = is the wavelet scale.

By varying the wavelet scale, s, and translating along the localized time index, n, one can generate a representation showing both the amplitude of any features versus the scale and how this amplitude varies with time. The subscript 0 on ψ has been dropped to indicate it has been normalized. Although it is possible to compute the wavelet transform using (6), Torrence and Campo [2] suggest it is faster to do the computations in Fourier space. By using all N points in the time series, the convolution theorem allows one to do all N convolutions simultaneously in Fourier space using a discrete Fourier transform (DFT). The DFT of time series x_n is:

$$\hat{x}_k = \frac{1}{N} \sum_{n=0}^{N-1} x_n e^{-2\pi i k n/N} , \qquad (7)$$

where,

 \hat{x}_k = is the DFT of the time-series

k = 0,..., N-1 is the frequency index.

In the continuous limit, the Fourier transform of a function of $\psi(t/s)$ is given by $\hat{\psi}(s\omega)$. By convolution theorem, the wavelet transform is the inverse Fourier transform of the product:

$$W_n(s) = \sum_{k=0}^{N-1} \hat{x}_k \hat{\psi} * (s\omega_k) e^{i\omega_k n \delta t} , \qquad (8)$$

where the angular frequency is defined as:

$$\omega_{k} = \begin{cases} \frac{2\pi k}{N\delta t} & : \quad k \le \frac{N}{2} \\ -\frac{2\pi k}{N\delta t} & : \quad k > \frac{N}{2} \end{cases}$$

$$(9)$$

Using (8) and a standard fast Fourier transform routine, one can calculate the continuous wavelet transform for all s at all n simultaneously and efficiently.

To ensure that the wavelet transforms (8) at each scale are directly compatible, the wavelet function at each scale is normalized to have unit energy:

$$\hat{\psi}(s\omega_k) = \left(\frac{2\pi s}{\delta t}\right)^{1/2} \hat{\psi}_0(s\omega_k) \,\, (10)$$

For the Morlet wavelet, the non-normalized Fourier transform of a function $\psi(t/s)$ is given by:

$$\hat{\psi}_0(s\omega_k) = \pi^{-1/4} H(\omega) e^{-(s\omega - \omega_0)^2/2}, \tag{11}$$

where,

 $H(\omega)$ = is the Heavyside step function; $H(\omega) = 1$ if $\omega > 0$, $H(\omega) = 0$ otherwise.

2.2 Wavelet Power Spectrum

In general, the wavelet transform is a complex number. This means that the transform can be divided into a real part (i.e., $\Re\{W_n(s)\}$) and an imaginary part (i.e., $\Im\{W_n(s)\}$). Alternatively, the transform can be divided into an amplitude (i.e., $|W_n(s)|$) and a phase (i.e., $\tan^{-1}[\Im\{W_n(s)\}/\Re\{W_n(s)\}]$). As suggested by Torrence and Campo [2], the wavelet power spectrum can be defined as $|W_n(s)|^2$ or normalized to $|W_n(s)|^2/\sigma^2$.

2.3 Choice of Scale

After choosing a wavelet function, it is necessary to choose a set of scales, s, to use in the wavelet transform. The scales can be written as fractional powers of two:

$$s_{j} = s_{0} 2^{j\delta j}, \quad j = 0, 1, ..., J$$
 (12)

$$J = \delta j^{-1} \log_2(N\delta t / s_0)$$
 (13)

where,

 s_0 = is the smallest resolvable scale, and

J = is an indicator of the largest possible scale.

The s_0 should be chosen so that the equivalent Fourier period is approximately $2\delta t$. The choice of a sufficiently small δj depends on the width in the spectral-space of the wavelet function. For the Morlet wavelet, a value δj of about 0.5 is the largest value that still gives adequate sampling in scale. Smaller values of δj give finer resolutions.

2.4 Wavelet Scale and Fourier Frequency

The maximum in $\hat{\psi}(s\omega)$ does not necessarily occur at a frequency of s⁻¹. Following the method presented by Meyers et al. [9], the correlation between the equivalent Fourier period and the wavelet scale can be derived for a particular wavelet function. This is done by substitution of a cosine wave of a known frequency into (8) and computing the scale, s, at which the wavelet power spectrum reaches its maximum. Torrence and Campo [2] have calculated that a Morlet wavelet with $\omega_0 = 6$, gives a value of $\lambda = 1.03$ s, where λ is the Fourier period. This indicates that for the Morlet wavelet the wavelet scale is almost equal to the Fourier period.

3. Methodology

A specific application of wavelet analysis is that it can be used to reduce the random uncertainty of nuclear thermalhydraulic time-series data. The methodology used to reduce the random uncertainty with wavelet analysis is presented in Figure 4.

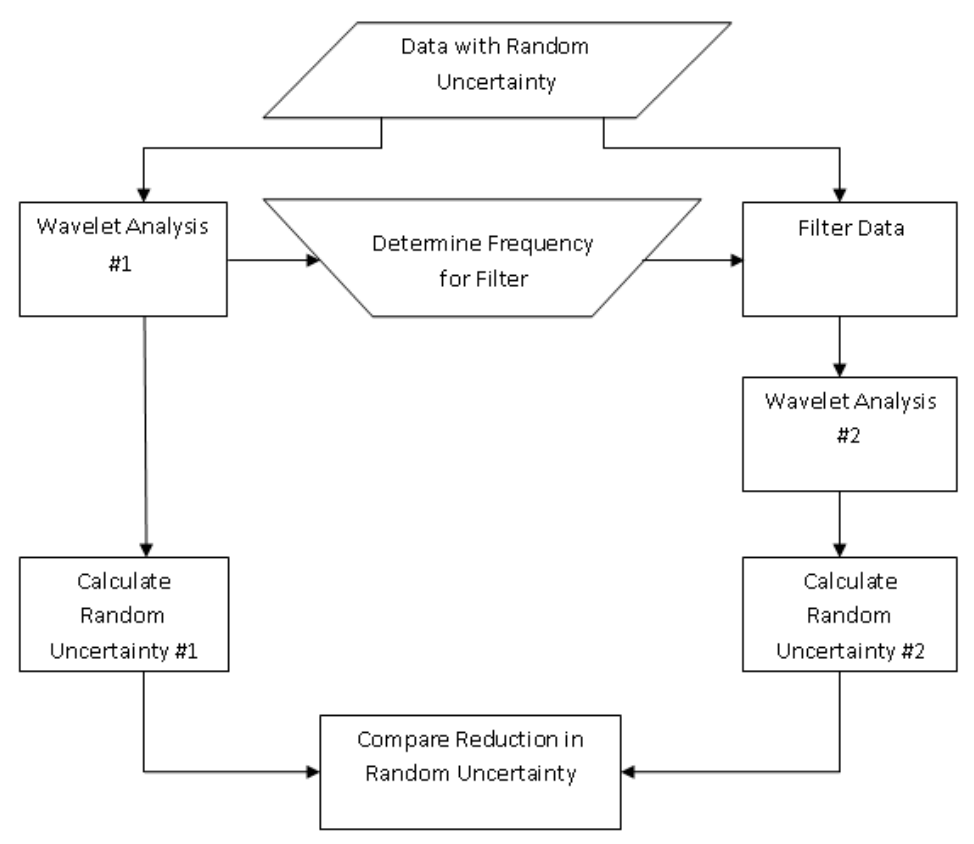


Figure 4: Random Uncertainty Reduction Methodology

First, nuclear thermalhydraulic time-series data with random uncertainty is analyzed using a wavelet transform. Upon examining the dominant modes of variability and how those modes vary in time, a passband frequency can be chosen such that it does not infringe upon the characteristic frequencies of the phenomenon being studied. Nonetheless, the frequency can be chosen such that it will filter the noisy part of the signal as much as possible. Once the frequency is chosen for the band-pass filter, it is used to filter the original time-series data. The filtered data can then be decomposed with the same wavelet transform into the time-series into the time-frequency domain for qualitative comparison purposes with the unfiltered data. The random uncertainties are then calculated and compared for both the filtered and unfiltered data for a quantitative indication of the reduction in uncertainty.

4. Results and Discussion

This section uses the methodology presented in section 3 to reduce the standard random uncertainty for an idealized measured void fraction time-series.

4.1 Wavelet Power Spectra and Data Filtering

The wavelet power spectrum for the idealized void fraction time-series data described in section 1.1 is shown in Figure 5. The void fraction transient shows a characteristic peak in the wavelet power spectrum at the time coinciding with the break.

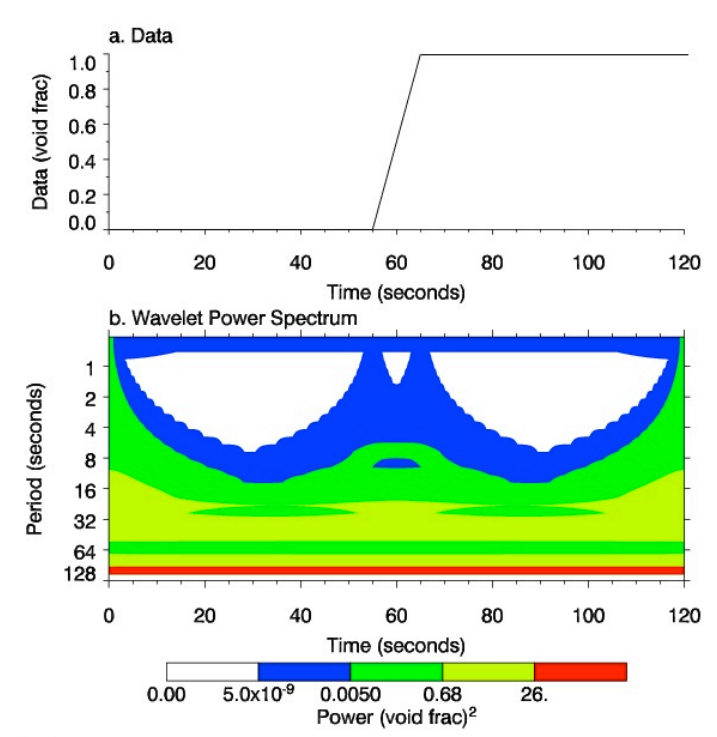


Figure 5: (a) "True" Time-Series Data. (b) The wavelet power spectrum. The contour levels are chosen so that 75%, 50%, 25%, and 5% of the wavelet power is above each level, respectively.

In contrast to Figure 5, Figure 6 shows the wavelet power spectrum for the measured void fraction time-series. The random uncertainty in the void fraction at any given point (i.e., $\pm 10\%$ void) contributes to the lower period region, i.e., higher frequency region, of the wavelet power spectrum. This validates the choice of a low band-pass digital filter to reduce the random uncertainty. Specifically, a fourth order low pass Butterworth filter was chosen to filter the measured data. As seen in Figure 6, a cutoff frequency of 0.125 Hz (i.e., period of 8 s) was chosen for the filter. This allows one to reduce the noise from the random uncertainty in the measured void fraction while preserving the characteristic frequencies of the phenomena during of the voiding transient. In other words, the voiding transient has a period of 10 seconds and choosing a period of less than 10 seconds (i.e., period of 8 s) does not remove any of the void fraction information.

Applying the filter to the data in Figure 6, yields to the time-series and wavelet power spectrum in Figure 7. Comparing these figures, reveals that the forth order low pass Butterworth does a good job of removing the high frequency noise caused by the random uncertainty while also preserving the characteristic frequencies of the voiding phenomena.

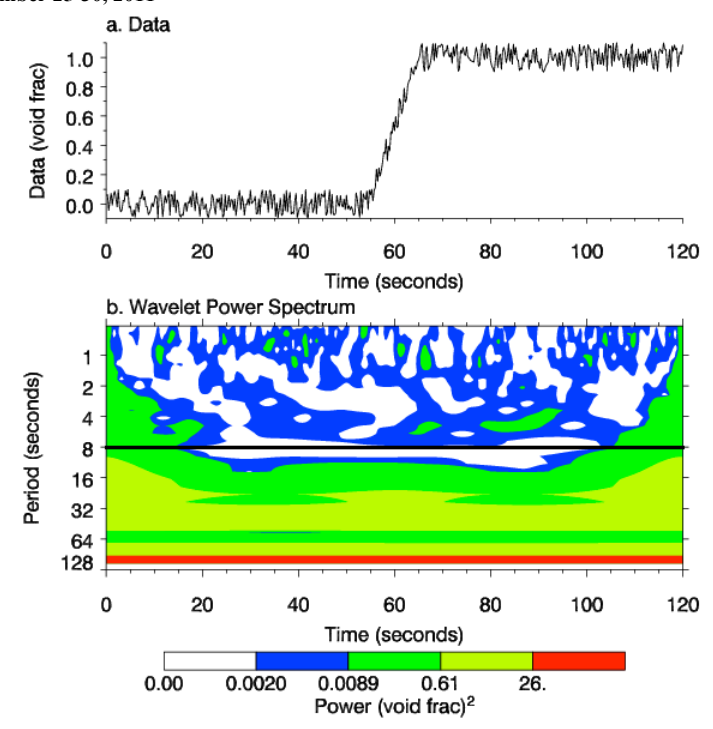


Figure 6: (a) "Measured" Time-Series Data. (b) The wavelet power spectrum. The contour levels are chosen so that 75%, 50%, 25%, and 5% of the wavelet power is above each level, respectively.

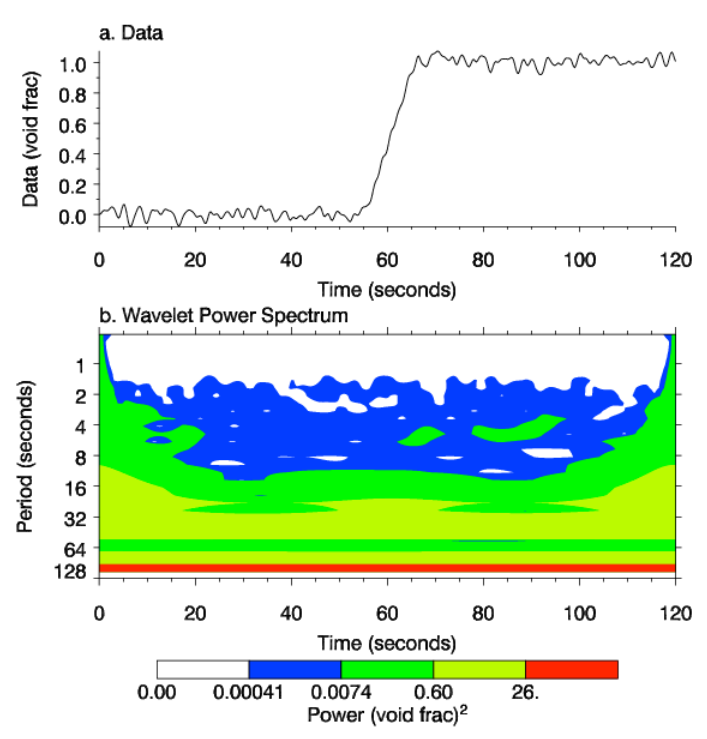


Figure 7: (a) Filtered Time-Series Data. (b) The wavelet power spectrum. The contour levels are chosen so that 75%, 50%, 25%, and 5% of the wavelet power is above each level, respectively.

4.2 Reduction in Uncertainty

To compare the uncertainties in the measured and filtered data sets on a consistent basis, i.e., relative to the true value, two different residuals can be defined. The measured residual is given by:

$$X_{measured,j} = \alpha_{measured,j} - \alpha_{true,j}, \tag{14}$$

where,

 $X_{measured.}$ = is the random residual error of the jth measurement,

 $\alpha_{measured,i}$ = is the jth measured void fraction value, and

 $\alpha_{true,j}$ = is the jth true void fraction value.

In essence, equation (14) is a measure of the distance between a measured value and the true value which can also be thought of as the random error in an individual measurement. Similarly, the distance between a filtered value and the true values can be defined as:

$$X_{filteredj} = \alpha_{filteredj} - \alpha_{true,j}, \tag{15}$$

where,

 $X_{filtered_i}$ = is the random residual error of jth filtered value,

 $\alpha_{filtered j}$ = is the jth filtered void fraction value, and

 $\alpha_{true,j}$ = is the jth true void fraction value.

Substituting (14) and (15) into (1) and calculating (2) and (3) in section 1.2 yields the values in Table 1.

Table 1: Uncertainty metrics for the measured and filtered data sets

Uncertainty Metric	Measured Data Set	Filtered Data Set
	(void fraction)	(void fraction)
Sample Mean	0.00700	0.00022
Sample Standard Deviation	0.05707	0.03289
Random Standard Uncertainty	0.00260	0.00150

The percentage reduction in the random standard uncertainty is provided by the following formula:

% reduction =
$$\frac{\left| \frac{S_{\overline{X}, f \text{ iltered}} - S_{\overline{X}, measured}}{S_{\overline{X}, measured}} \right| \times 100,$$
 (16)

where,

 $s_{\overline{X}, f illered}$ = is the standard random uncertainty for the filtered data set, and

 $s_{\overline{X},measured}$ = is the standard random uncertainty for the filtered data set.

The percent reduction in the random standard uncertainty is approximately 42.4%.

5. Conclusions

Wavelet transforms and wavelet analysis has been shown to be a valuable time-series analysis tool in the field of nuclear thermalhydraulics. As a proof of concept, the Morlet wavelet transform was used in an uncertainty reduction technique aimed at the reducing the aleatory uncertainty of a voiding transient in a large loss of coolant accident (LOCA). The wavelet transform enabled the choice of cutoff frequency (0.125 Hz) for a low pass forth order Butterworth filter in order to remove the noisy part of the signal without infringing upon the characteristic frequencies for this specific phenomenon (i.e., the idealized voiding transient). This technique facilitated a 42.4% reduction in the standard random uncertainty.

6. References

- [1] M.H. Trauth, MATLAB Recipes for Earth Sciences, Springer, 2007, pp. 114-119.
- [2] C. Torrence and G.P. Compo, "A Practical Guide to Wavelet Analysis", Bulletin of the American Meteorological Society, Vol. 79, No. 1, January 1998, pp. 61-78.
- [3] K.M. Lau and H. Weng, "Climate Signal Detection Using Wavelet Transform: How to Make a Time Series Sing", Bulletin of the American Meteorological Society, Vol. 76, No. 13, December 1995, pp. 2391-2402.
- [4] AMSE PTC 19.1-2005, "Test Uncertainty", The American Society of Mechanical Engineers, 2006.
- [5] IAEA-TECDOC-1395, "Intercomparison and Validation of computer codes for thermalhydraulic safety analysis of heavy water reactors", International Atomic Energy Agency, August 2004.
- [6] J.R. Buell, D.P Byskal, M.R. Desrosiers, E.M.A. Hussein, P.J. Ingham and R.S. Swartz, "A neutron scatterometer for void-fraction measurement in heated rod-bundle channels under CANDU LOCA conditions", International Journal of Multiphase Flow, Vol. 31, No. 4, April 2005, pp. 452-472.
- [7] S. Butterworth, "On the Theory of Filter Amplifiers", Wireless Engineer, Vol. 7, pp. 536–541, October 1930.
- [8] C. Torrence and G.P. Compo, "A Practical Guide to Wavelet Analysis", Internet: http://paos.colorado.edu/research/wavelets/, [March 27, 2011].
- [9] S.D. Meyers, B. G. Kelly, and J. J. O'Brien, "An introduction to wavelet analysis in oceanography and meteorology: With application to the dispersion of Yanai waves", Mon. Wea. Rev., Vol. 121, No. 10, pp. 2858–2866, October 1993.